

CP Violation in $D^0 \rightarrow K_S K_S$

Ulrich Nierste^{a*} and Stefan Schacht^{a†}

^a *Institut für Theoretische Teilchenphysik, Karlsruher Institut für Technologie, 76128 Karlsruhe, Germany*

The direct CP asymmetry $a_{CP}^{\text{dir}}(D^0 \rightarrow K_S K_S)$ involves exchange diagrams which are induced at tree level in the Standard Model. Since the corresponding topological amplitude E_{KK} can be large, $D^0 \rightarrow K_S K_S$ is a promising discovery channel for charm CP violation. We estimate the penguin annihilation amplitude with a perturbative calculation and extract the exchange amplitude E_{KK} from a global fit to D branching ratios. Our results are further used to predict the size of mixing-induced CP violation. We obtain $|a_{CP}^{\text{dir}}(D^0 \rightarrow K_S K_S)| \leq 1.1\%$ (95% C.L.). The same bound applies to the nonuniversal part of the phase between the $D-\bar{D}$ mixing and decay amplitudes. If future data exceed our predictions, this will point to new physics or an enhancement of the penguin annihilation amplitude by QCD dynamics. We briefly discuss the implications of these possibilities for other CP asymmetries.

I. INTRODUCTION

While direct CP violation (CPV) is well established in the down-quark sector [1–11], CPV has not yet been observed in the decays of up-type quarks. For the discussion of CPV in some singly Cabibbo-suppressed D decay it is convenient to decompose the decay amplitude \mathcal{A} as

$$\mathcal{A} = \lambda_{sd} \mathcal{A}_{sd} - \frac{\lambda_b}{2} \mathcal{A}_b. \quad (1)$$

Here $\lambda_q \equiv V_{cq}^* V_{uq}$ and $\lambda_{sd} = (\lambda_s - \lambda_d)/2$ comprise the elements V_{ij} of the Cabibbo-Kobayashi-Maskawa (CKM) matrix. In the limit $\lambda_b = 0$ all direct and mixing-induced CP asymmetries vanish in the Standard Model (SM). The suppression factor $\text{Im} \frac{\lambda_b}{\lambda_{sd}} \sim -6 \cdot 10^{-4}$ makes the discovery of CKM-induced CPV challenging. At the same time this parametric suppression renders CP asymmetries in charm decays highly sensitive to physics beyond the SM.

In this paper we study the decay $D^0 \rightarrow K_S K_S$. For this decay mode \mathcal{A}_{sd} vanishes in the limit of exact $SU(3)_F$ symmetry [12–15], so that the branching ratio is suppressed. However, \mathcal{A}_b does not vanish in this limit and we expect $|\mathcal{A}_b/\mathcal{A}_{sd}|$ to be large. Therefore CP asymmetries in $D^0 \rightarrow K_S K_S$ may be enhanced to an observable level, even if the Kobayashi-Maskawa phase is the only source of CPV in charm decays [14, 15]. Moreover, a special feature of $D^0 \rightarrow K_S K_S$ is the interference of the decays $c\bar{u} \rightarrow \bar{s}s$ and $c\bar{u} \rightarrow \bar{d}d$, both of which involve the tree-level exchange of a W boson (exchange topology E , see Fig. 1). This interference term gives a contribution to \mathcal{A}_b owing to $\lambda_d + \lambda_s = -\lambda_b$. That is, contrary to the widely studied decays $D \rightarrow \pi^+\pi^-, \pi^0\pi^0, K^+K^-$, no penguin diagrams are needed for nonzero direct or mixing-induced CP asymmetries. Moreover, the exchange diagram E is

enhanced by a large Wilson coefficient. These properties make $D^0 \rightarrow K_S K_S$ an interesting discovery channel for CPV in the charm system.

In this paper we calculate the allowed ranges for the direct and mixing-induced CP asymmetries in $D^0 \rightarrow K_S K_S$, using the results of our global analysis in Ref. [16]. There are two ingredients which we cannot extract from this analysis: the first one is the penguin-annihilation amplitude PA (see Fig. 1), which we estimate with the help of a perturbative calculation. The other undetermined quantity is a strong phase δ , whose value, however, can be determined from the data once both the direct and mixing-induced CP asymmetries are measured. The actual size of δ is not crucial for the potential to discover charm CPV in $D^0 \rightarrow K_S K_S$: depending on whether $|\sin \delta|$ is large or small either the direct or mixing-induced CP asymmetry will be large.

Our paper is organized as follows: in Section II we derive handy formulae for direct and mixing-induced CP asymmetries in terms of \mathcal{A}_{sd} and \mathcal{A}_b . In Section III we relate the CPV observables to topological amplitudes. Subsequently we estimate the penguin annihilation contribution, which cannot be extracted from a global fit to current data, with perturbative methods in Section IV. In Section V we present our phenomenological analysis. Finally, we conclude.

II. PRELIMINARIES

In this section we collect the formulae for the CP asymmetries. We write

$$\mathcal{A}(D^0 \rightarrow K_S K_S) = -\frac{1}{\sqrt{2}} \mathcal{A}(D^0 \rightarrow \bar{K}^0 K^0), \quad (2)$$

accommodating the Bose symmetrization of the two K_S 's with the factor of $1/\sqrt{2}$. Here we identify $K_S = (K^0 - \bar{K}^0)/\sqrt{2}$ and assume that the effects of kaon CPV are

* ulrich.nierste@kit.edu

† stefan.schacht@kit.edu

properly subtracted from CP asymmetries measured in $D^0 \rightarrow K_S K_S$, as described in Ref. [17]. Adopting the convention $CP|D^0\rangle = -|\bar{D}^0\rangle$ [18] the amplitude of $\bar{D}^0 \rightarrow K_S K_S$ is

$$\bar{\mathcal{A}} = -\lambda_{sd}^* \mathcal{A}_{sd} + \frac{\lambda_b^*}{2} \mathcal{A}_b. \quad (3)$$

The direct CP asymmetry reads

$$a_{CP}^{\text{dir}} \equiv \frac{|\mathcal{A}|^2 - |\bar{\mathcal{A}}|^2}{|\mathcal{A}|^2 + |\bar{\mathcal{A}}|^2} \quad (4)$$

$$= \frac{\text{Im} \lambda_b}{|\mathcal{A}|} \text{Im} \frac{\mathcal{A}_b}{\mathcal{A}_{sd}} |\mathcal{A}_{sd}|. \quad (5)$$

Here and in the following we neglect terms of order λ_b^2 and higher. Furthermore we use the PDG convention for the CKM elements, so that λ_{sd} is real and positive up to corrections of order λ_b .

For the discussion of mixing-induced CPV we also follow the conventions of Ref. [18]: with the mass eigenstates $|D_{1,2}\rangle = p|D^0\rangle \pm q|\bar{D}^0\rangle$ we define the weak phase ϕ governing CPV in the interference between the $D-\bar{D}$ mixing and the $D^0 \rightarrow K_S K_S$ decay through

$$\begin{aligned} \frac{q}{p} \frac{\bar{\mathcal{A}}}{\mathcal{A}} &= -\frac{q}{p} \frac{\lambda_{sd}^*}{\lambda_{sd}} \frac{1 - \frac{\lambda_b^*}{2\lambda_{sd}^*} \frac{\mathcal{A}_b}{\mathcal{A}_{sd}}}{1 - \frac{\lambda_b}{2\lambda_{sd}} \frac{\mathcal{A}_b}{\mathcal{A}_{sd}}} \\ &\equiv \left| \frac{q}{p} \right| \left| \frac{\bar{\mathcal{A}}}{\mathcal{A}} \right| e^{i\phi}. \end{aligned} \quad (6)$$

In this paper we focus on CPV effects which are specific to the decay $D^0 \rightarrow K_S K_S$. It is therefore useful to define a CP phase ϕ_{mix} which enters all mixing-induced CP asymmetries in a universal way:

$$-\frac{q}{p} \frac{\lambda_{sd}^*}{\lambda_{sd}} \equiv \left| \frac{q}{p} \right| e^{i\phi_{\text{mix}}}. \quad (7)$$

Comparing Eqs. (6) and (7) one verifies that ϕ_{mix} coincides with ϕ if one sets λ_b to zero in $\bar{\mathcal{A}}/\mathcal{A}$. In the hunt for new physics (NP) in $D-\bar{D}$ mixing, which may well enhance ϕ_{mix} over the SM expectation $\phi_{\text{mix}} = \mathcal{O}(\text{Im} \lambda_b/\lambda_{sd})$, one fits the CPV data of all available D^0 decays to a common phase ϕ_{mix} [19, 20]. In the case of $D^0 \rightarrow K_S K_S$, however, we face the possibility that already the SM contributions lead to the situation $|\phi| \gg |\phi_{\text{mix}}|$. Comparing Eq. (6) with Eq. (7) one finds

$$\begin{aligned} \frac{1 - \frac{\lambda_b^*}{2\lambda_{sd}^*} \frac{\mathcal{A}_b}{\mathcal{A}_{sd}}}{1 - \frac{\lambda_b}{2\lambda_{sd}} \frac{\mathcal{A}_b}{\mathcal{A}_{sd}}} &= \left| \frac{\bar{\mathcal{A}}}{\mathcal{A}} \right| e^{i(\phi - \phi_{\text{mix}})} \\ &= (1 - a_{CP}^{\text{dir}}) e^{i(\phi - \phi_{\text{mix}})}, \end{aligned} \quad (8)$$

where we have used Eq. (4), discarding higher-order terms $\sim (a_{CP}^{\text{dir}})^2$ as usual. By expanding Eq. (8) to first

order in λ_b and $\phi - \phi_{\text{mix}}$ we arrive at

$$\phi - \phi_{\text{mix}} = \text{Im} \frac{\lambda_b}{\lambda_{sd}} \text{Re} \frac{\mathcal{A}_b}{\mathcal{A}_{sd}} = \frac{\text{Im} \lambda_b}{|\mathcal{A}|} \text{Re} \frac{\mathcal{A}_b}{\mathcal{A}_{sd}} |\mathcal{A}_{sd}|. \quad (9)$$

Eqs. (5) and (9) form the basis of the analysis presented in the following sections. In Eqs. (5) and (9) $|\mathcal{A}|$ is trivially related to the well-measured branching ratio:

$$\begin{aligned} |\mathcal{A}| &= \sqrt{\frac{\mathcal{B}(D \rightarrow K_S K_S)}{\mathcal{P}(D, K, K)}}, \\ \mathcal{P}(D, K, K) &\equiv \tau \frac{1}{16\pi m_D^2} \sqrt{m_D^2 - 4m_{K^0}^2}, \end{aligned} \quad (10)$$

The experimental value is $\mathcal{B}(D^0 \rightarrow K_S K_S) = (0.17 \pm 0.04) \cdot 10^{-3}$ [21]. The nontrivial quantities entering the predictions of a_{CP}^{dir} and $\phi - \phi_{\text{mix}}$ are \mathcal{A}_b and the phase of \mathcal{A}_{sd} .

The time-dependent CP asymmetry reads

$$\begin{aligned} A_{CP}(t) &= \frac{\Gamma(D^0(t) \rightarrow K_S K_S) - \Gamma(\bar{D}^0(t) \rightarrow K_S K_S)}{\Gamma(D^0(t) \rightarrow K_S K_S) + \Gamma(\bar{D}^0(t) \rightarrow K_S K_S)} \\ &= a_{CP}^{\text{dir}} - A_\Gamma \frac{t}{\tau}. \end{aligned} \quad (11)$$

Here τ is the D^0 lifetime and

$$A_\Gamma = \left[\frac{1}{2} \left(\left| \frac{q}{p} \right|^2 - 1 \right) - a_{CP}^{\text{dir}} \right] y \cos \phi - x \sin \phi. \quad (12)$$

Eq. (12) contains the mass difference ΔM and the width difference $\Delta\Gamma$ between the mass eigenstates D_1 and D_2 through $x = \tau\Delta M$ and $y = \tau\Delta\Gamma/2$. In Eqs. (11) and (12) all quadratic (and higher) terms in tiny quantities are neglected. In time-integrated measurements, LHCb measures the quantity [18, 22, 23]

$$A_{CP} = a_{CP}^{\text{dir}} - A_\Gamma \frac{\langle t \rangle}{\tau}, \quad (13)$$

where $\langle t \rangle$ is the average decay time. CLEO has measured [24]

$$A_{CP}^{\text{CLEO}} = -0.23 \pm 0.19. \quad (14)$$

Recently LHCb has reported the preliminary result [25]

$$A_{CP}^{\text{LHCb}} = -0.029 \pm 0.052 \pm 0.022. \quad (15)$$

III. TOPOLOGICAL AMPLITUDES

The decomposition of \mathcal{A}_{sd} and \mathcal{A}_b in terms of topological amplitudes reads [16]

$$\mathcal{A}_{sd} = \frac{E_1 + E_2 - E_3}{\sqrt{2}}, \quad (16)$$

$$\mathcal{A}_b = \frac{2E + E_1 + E_2 + E_3 + PA}{\sqrt{2}} \quad (17)$$

$$= -\mathcal{A}_{sd} + \frac{2E_{KK} + PA}{\sqrt{2}}. \quad (18)$$

Here $E_{KK} \equiv E + E_1 + E_2$ is the combination of exchange diagrams appearing in $D^0 \rightarrow K^+K^-$. The exchange (E) and penguin annihilation (PA) diagrams are shown in Fig. 1. $E_{1,2,3}$ account for first-order $SU(3)_F$ breaking in diagrams containing s -quark lines (for their precise definition see Table II of Ref. [16]). As in Ref. [26] PA_q denotes the penguin annihilation diagram with quark q running in the loop. We use the combinations [15, 27, 28]

$$\begin{aligned} & \lambda_s PA_s + \lambda_d PA_d + \lambda_b PA_b = \\ & \lambda_{sd}(PA_s - PA_d) + \frac{\lambda_s + \lambda_d}{2} (PA_s + PA_d - 2PA_b) \end{aligned} \quad (19)$$

$$\equiv \lambda_{sd} PA_{\text{break}} - \frac{\lambda_b}{2} PA. \quad (20)$$

We recall that E , $E_{1,2,3}$, PA, \dots are defined for $D^0 \rightarrow K^0\bar{K}^0$ or $D^0 \rightarrow K^+K^-$. Since \mathcal{A}_{sd} and \mathcal{A}_b instead involve $K_S K_S$, the factor of $-1/\sqrt{2}$ of Eq. (2) appears in Eqs. (16) to (18).

Next we define the strong phase

$$\delta \equiv \arg \left(\frac{2E_{KK} + PA}{\mathcal{A}_{sd}} \right), \quad (21)$$

and the positive quantity

$$R = -\frac{\text{Im}\lambda_b}{|\mathcal{A}|} \frac{|2E_{KK} + PA|}{\sqrt{2}}. \quad (22)$$

With Eq. (18) we can write Eq. (9) as

$$\begin{aligned} \phi - \phi_{\text{mix}} &= \text{Im} \frac{\lambda_b}{\lambda_{sd}} \text{Re} \frac{-\mathcal{A}_{sd} + (2E_{KK} + PA)/\sqrt{2}}{\mathcal{A}_{sd}} \\ &= -\text{Im} \frac{\lambda_b}{\lambda_{sd}} - R \cos \delta. \end{aligned} \quad (23)$$

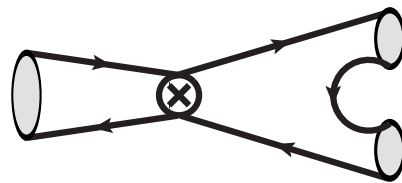
In the same way one finds

$$a_{CP}^{\text{dir}} = -R \sin \delta. \quad (24)$$

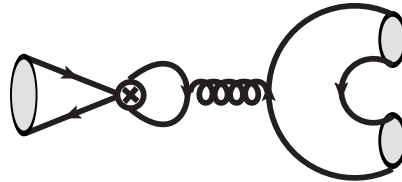
Eqs. (23) and (24) mean that a_{CP}^{dir} and $\phi - \phi_{\text{mix}}$ lie on a circle with radius R centered at $(-\text{Im} \frac{\lambda_b}{\lambda_{sd}}, 0)$. The allowed points are parametrized by the phase δ , which we cannot predict. The actual value of δ , however, is of minor importance for the discovery potential of CPV, because δ only controls how the amount of CPV is shared between a_{CP}^{dir} and $\phi - \phi_{\text{mix}}$. The crucial parameter is R , which determines the maximal values of $|a_{CP}^{\text{dir}}|$ and $|\phi - \phi_{\text{mix}}|$. Once a_{CP}^{dir} and $\phi - \phi_{\text{mix}}$ are precisely measured one can determine R through

$$R = \sqrt{a_{CP}^{\text{dir}2} + \left(\phi - \phi_{\text{mix}} + \text{Im} \frac{\lambda_b}{\lambda_{sd}} \right)^2}. \quad (25)$$

The experimental value can then be confronted with the theoretical estimate presented in the next section. The impact of our estimate on a_{CP}^{dir} and $\phi - \phi_{\text{mix}}$ will be presented below in Fig. 4.



(a)



(b)

FIG. 1. Topological amplitudes: (a) exchange (E) and (b) penguin annihilation (PA). Ref. [29] claims that $D^0 \rightarrow K_S K_S$ is Zweig suppressed, but this statement is only true for the PA diagram.

IV. ESTIMATE OF $|PA|$ AND R

The quantity $|E_{KK}|$ can be determined from our global fit to branching ratios [16]. For the calculation of PA we exploit the large momentum $\sqrt{q^2} \sim 1.5 \text{ GeV}$ flowing through the penguin loop in Fig. 1(b) and calculate this loop perturbatively as in Ref. [14]. Such methods are routinely used in B physics [30–35], but their applicability to charm physics is not clear.

We work in a five-flavor theory, so that only current-current operators appear in the effective Hamiltonian. With $Q_2 \equiv (\bar{u}s)_{V-A}(\bar{s}c)_{V-A} + (\bar{u}d)_{V-A}(\bar{d}c)_{V-A} - 2(\bar{u}b)_{V-A}(\bar{b}c)_{V-A}$ and the Wilson coefficient $C_2 \sim 1.2$ we may write

$$\mathcal{A}_b = \frac{G_F}{\sqrt{2}} C_2 \langle K_S K_S | Q_2 | D^0 \rangle, \quad (26)$$

because the contribution of the color-flipped operator Q_1 is highly suppressed. For our estimate of the ratio PA/E_{KK} in this section we adopt the $SU(3)_F$ limit and identify E_{KK} with E . In this limit we can combine Eqs. (26) and (17) into

$$\frac{G_F}{\sqrt{2}} C_2 \langle K_S K_S | Q_2 | D^0 \rangle = \frac{2E + PA}{\sqrt{2}}. \quad (27)$$

The penguin diagram can be written as [36]

$$\begin{aligned} PA &= G_F \frac{\alpha_s}{4\pi} C_2 \times \\ &\times \sum_{i=3}^6 (r_{2i}^d + r_{2i}^s - 2r_{2i}^b) \langle K_S K_S | Q_i | D^0 \rangle, \end{aligned} \quad (28)$$

with the loop function $r_{24}^q \equiv r_{24}^q(q^2, m_q^2, \mu^2) = r_{26}^q$ defined in Ref. [36]. $\mu \sim \sqrt{q^2}$ is the renormalization scale which

also enters α_s and C_2 in Eq. (28). Q_{3-6} are the usual four-quark penguin operators, we will need

$$Q_{4,6} = (\bar{u}^\alpha c^\beta)_{V-A} \sum_{q=u,d,s,c,b} (\bar{q}^\beta q^\alpha)_{V\mp A}. \quad (29)$$

PA is color-suppressed w.r.t. E and this suppression is encoded in Eq. (28) through $\alpha_s \sim 1/N_c$. The contributions from the matrix elements $\langle Q_{3,5} \rangle$ are further suppressed and are neglected in the following. We write $\langle Q_4 \rangle + \langle Q_6 \rangle = -2(M_{VA}^d + M_{VA}^s)$ with

$$M_{VA}^q \equiv \langle K_S K_S | (\bar{q}_\alpha q_\beta)_V (\bar{u}_\beta c_\alpha)_A | D^0 \rangle. \quad (30)$$

The other quark flavors in the sum in Eq. (29) contribute to $D^0 \rightarrow K_S K_S$ only through another loop diagram, yielding a contribution of higher order in α_s . With

$$p \equiv r_{24}^d + r_{24}^s - 2r_{24}^b, \quad (31)$$

we can write PA in a compact form:

$$PA = -G_F \frac{\alpha_s}{\pi} C_2 p M_{VA}^d, \quad (32)$$

where we have invoked the $SU(3)_F$ limit to set $M_{VA}^d = M_{VA}^s$. The μ -dependence cancels in p , which furthermore does not depend on m_c in the considered leading order. It is an excellent numerical approximation to expand p to first order in m_s^2/q^2 and q^2/m_b^2 (while setting $m_d = 0$). The expanded expression reads

$$p = -\frac{10}{9} - \frac{2}{3}i\pi - \frac{2m_s^2}{q^2} + \frac{2q^2}{15m_b^2} + \frac{2}{3} \ln \frac{q^2}{m_b^2}. \quad (33)$$

It is worthwhile to discuss how this result translates into an expression in a four-flavor theory, in which the b quark is integrated out at the scale $\mu_b = \mathcal{O}(m_b)$: in this alternative approach the piece $-2r_{24}^b$ of Eq. (28) resides in the initial conditions of the penguin coefficients C_{3-6} generated at μ_b . The four-flavor theory permits the use of the renormalization group (RG) to resum the $\log \ln(\mu_b/\sqrt{q^2})$ to all orders in perturbation theory, but this resummation is inconsistent since $\ln(\mu_b/\sqrt{q^2})$ is smaller than the nonlogarithmic terms in $-2r_{24}^b$. Without RG summation the four-flavor theory reproduces exactly the analytic result in Eq. (33), which is independent of renormalization scale and scheme.

To estimate M_{VA}^d we want to relate it to E using Eq. (27). After Fierz-rearranging Q_2 we can express the LHS of Eq. (27) in terms of M_{VA}^q and

$$M_{AV}^q \equiv \langle K_S K_S | (\bar{q}_\alpha q_\beta)_A (\bar{u}_\beta c_\alpha)_V | D^0 \rangle. \quad (34)$$

The exchange topology reads (cf. Eq. (27))

$$\begin{aligned} E &= G_F C_2 \langle K_S K_S | (\bar{u}d)_{V-A} (\bar{d}c)_{V-A} | D^0 \rangle - PA_d \\ &= -G_F C_2 (M_{AV}^d + M_{VA}^d) - G_F \frac{\alpha_s}{\pi} C_2 r_{24}^d M_{VA}^d. \end{aligned} \quad (35)$$

To leading order in α_s we have therefore $E = -G_F C_2 (M_{AV}^d + M_{VA}^d)$. For the desired estimate of

PA/E we need M_{VA}^d/E . We can place a bound on this quantity with Eq. (35), if we assume that $|M_{VA}^d|$ is not much larger than $|M_{AV}^d + M_{VA}^d|$; i.e. we do not consider the case of large cancellations between M_{AV}^d and M_{VA}^d in E . In view of the fact that E is numerically large [16] this assumption seems justified. Writing

$$M_{VA}^d = \kappa (M_{AV}^d + M_{VA}^d), \quad (36)$$

we vary $|\kappa|$ between 0 and 2. Now Eq. (35) entails

$$\frac{M_{VA}^d}{E} = \frac{\kappa}{-G_F C_2 (1 + \kappa \frac{\alpha_s}{\pi} r_{24}^d)}, \quad (37)$$

and thus

$$|2E_{KK} + PA| = |2E_{KK}| \left| 1 + \frac{\alpha_s}{2\pi} p \frac{\kappa}{1 + \kappa \frac{\alpha_s}{\pi} r_{24}^d} \right| \quad (38)$$

$$\leq |2E_{KK}| \times 1.3, \quad (39)$$

Here we have used $\mu = \sqrt{q^2} = 1.5$ GeV, $m_s(\mu) = 0.104$ GeV, $m_b(\mu) = 4.18$ GeV, and $\alpha_s(\mu) = 0.328$. (r_{24}^d is evaluated in the NDR scheme.) Inserting finally Eq. (39) into Eq. (22) gives the upper limit

$$R \leq -1.3 \frac{\text{Im} \lambda_b}{|\lambda|} \frac{|2E_{KK}|}{\sqrt{2}}. \quad (40)$$

This bound determines the radius of the circle which defines the allowed area for $(\phi - \phi_{\text{mix}}, a_{CP}^{\text{dir}})$ via Eq. (25). I.e. Eq. (40) determines the maximal size of both $|a_{CP}^{\text{dir}}|$ and $|\phi - \phi_{\text{mix}}|$ (neglecting the small $\text{Im} \lambda_b/\lambda_{sd}$ in Eq. (23)). If future data violate Eq. (40), this will signal new physics or a dynamical enhancement of PA over the perturbative result in Eq. (32). Sec. V discusses how these two scenarios can be distinguished with the help of other measurements.

The relation of $r_{24}^q(q^2, m_q^2, \mu^2)$ to $G(s, x)$ in Ref. [32] is given as

$$\begin{aligned} r_{24}^q(q^2, m_q^2, \mu^2) &= \frac{1}{3} - \frac{1}{3} \log \left(\frac{\mu^2}{m^2} \right) \\ &\quad - \frac{1}{2} G \left(\frac{m_q^2 - i\varepsilon}{m^2}, \frac{q^2}{m^2} \right), \end{aligned} \quad (41)$$

with an arbitrary mass m^2 . Note that the $-i\varepsilon$ prescription is essential here; an erroneous omission of this small imaginary part results in a numerically large mistake. The prefactor of $G(x, y)$ in Eq. (41) disagrees with Ref. [14]. We further find that the b -quark contribution $-2r_{24}^b$ is numerically as important as $r_{24}^d + r_{24}^s$:

$$r_{24}^d(q^2, 0, \mu^2) = -0.22 - i 1.05, \quad (42)$$

$$r_{24}^s(q^2, m_s^2, \mu^2) = -0.23 - i 1.05, \quad (43)$$

$$-2r_{24}^b(q^2, m_b^2, \mu^2) = -2.02. \quad (44)$$

	with $1/N_c$		without $1/N_c$	
	$PA = 0$	$PA \neq 0$	$PA = 0$	$PA \neq 0$
$ E_{KK}/T^{\text{fac}} \leq$	1.5		2.6	
$R \leq$	0.004	0.006	0.009	0.011

TABLE I. 95% C.L. upper limits ($\Delta\chi^2 = 3.84$), with or without $1/N_c$ input for C and E .

V. PHENOMENOLOGY

The last element needed for the calculation of our bound in Eq. (40) is $|E_{KK}|$. To find $|E_{KK}|$ we employ our global fit to all available branching ratios of D decays to two pseudoscalar mesons [16]. Note that the main constraint on this quantity stems from $\mathcal{B}(D^0 \rightarrow K^+K^-)$ (see Table III of Ref. [16]). The D decays entering our fit involve other topological amplitudes in addition to E and PA ; in the following we refer to the color-favored tree (T), color-suppressed tree (C), annihilation (A) and penguin (P) amplitudes.

We consider two scenarios: in the first scenario the $SU(3)_F$ -limit amplitudes C and E are varied completely freely. In the second scenario we apply $1/N_c$ counting [37–39] to the amplitudes, where $N_c = 3$ is the number of colors. To leading order in $1/N_c$ one can factorize T which results in

$$T^{\text{fac}} \equiv \frac{G_F}{\sqrt{2}} a_1 f_\pi (m_D^2 - m_\pi^2) F_0^{D\pi}(m_\pi^2). \quad (45)$$

Here $a_1 = 1.06$ is the appropriate combination of Wilson coefficients, m_π and f_π are the mass and the decay constant of the pion, respectively, and $F_0^{D\pi}$ is the appropriate $D \rightarrow \pi$ form factor. (Recall that the $SU(3)_F$ -limit amplitudes are defined for decays into pions.) In our second scenario we assume that $|(C + \delta_A)/T^{\text{fac}}|$, $|(E + \delta_A)/T^{\text{fac}}| \leq 1.3$ [26], where δ_A parametrizes $1/N_c^2$ corrections to the factorized annihilation (A) topology [16].

The $\Delta\chi^2$ -profile of $|E_{KK}/T^{\text{fac}}|$ returned by our global fit is shown in Fig. 2(a). Fig. 2(b) shows the $\Delta\chi^2$ -profile of R for the special case $PA = 0$, in which the whole effect comes from the exchange diagram E_{KK} . The corresponding 95% C.L. bounds on $|E_{KK}/T^{\text{fac}}|$ and R inferred from Fig. 2 and Eq. (40) are given in Table I and illustrated in Fig. 3. Note that we do not treat T^{fac} as constant, but also fit the form factor $F_0^{D\pi}$. Likewise our fit permits $\mathcal{B}(D^0 \rightarrow K_S K_S)$ to float within the experimental errors.

Fig. 4 condenses the main results of this paper into a single plot: the radial lines correspond to fixed values of the strong phase δ in Eqs. (23) and (24) in the $\phi - \phi_{\text{mix}} - a_{CP}^{\text{dir}}$ plane. The red and blue discs show the allowed regions for the two considered scenarios. Note that our bounds depend on branching ratio measurements only and do not involve correlations to other CP asymmetries. The black circles correspond to different values

of $|2E_{KK} + PA|$ in Eq. (22). Future data on $\phi - \phi_{\text{mix}}$ and a_{CP}^{dir} will allow us to determine δ and R . The experimental value of R can then be confronted with the upper limits in Table I to probe the color counting in E_{KK} and our estimate of PA . New physics will mimic a dynamical enhancement of PA . In case an anomalously large value of R will be found, one can proceed in the following way to discriminate between different explanations:

- (i) Several CP asymmetries involve PA , but do not grow with $|E|$. For example,

$$\begin{aligned} a_{CP}^{\text{dir}}(D^0 \rightarrow K^+K^-), a_{CP}^{\text{dir}}(D^0 \rightarrow \pi^+\pi^-), \\ a_{CP}^{\text{dir}}(D^0 \rightarrow \pi^0\pi^0), \end{aligned} \quad (46)$$

all depend on $P + PA$ and are expected to be enhanced with PA as well, unless the increase is compensated by $-P$. But in this case instead

$$\begin{aligned} a_{CP}^{\text{dir}}(D^+ \rightarrow K_S K^+), a_{CP}^{\text{dir}}(D_s^+ \rightarrow K_S \pi^+), \\ a_{CP}^{\text{dir}}(D_s^+ \rightarrow K^+ \pi^0), \end{aligned} \quad (47)$$

which involve P rather than $P + PA$, become large. Thus a breakdown of color counting in E_{KK} can be distinguished from an enhanced PA .

- (ii) PA can be enhanced by QCD dynamics or by new physics. In the first case the CP asymmetries in Eqs. (46) and (47) will still obey the sum rules of Ref. [26]. New physics will violate these sum rules if it couples differently to down and strange quarks.

We close this section by comparing our result with other estimates of $a_{CP}^{\text{dir}}(D^0 \rightarrow K_S K_S)$ in the literature. Using generic $SU(3)_F$ counting Ref. [14] quotes

$$|a_{CP}^{\text{dir}}(D^0 \rightarrow K_S K_S)| \lesssim \frac{2|V_{cb}V_{ub}|}{\varepsilon|V_{cs}V_{us}|} \sim 0.6\%, \quad (48)$$

where ε quantifies $SU(3)_F$ breaking. Our result in Table I agrees with this estimate. However, if the possibility of a large, $1/N_c$ -unsuppressed $|E_{KK}|$ is realized in nature, $|a_{CP}^{\text{dir}}|$ can be twice as large.

Ref. [15] relates $a_{CP}^{\text{dir}}(D^0 \rightarrow K_S K_S)$ to $\Delta a_{CP}^{\text{dir}} \equiv a_{CP}^{\text{dir}}(K^+K^-) - a_{CP}^{\text{dir}}(\pi^+\pi^-)$. With present data this relation reads

$$|a_{CP}^{\text{dir}}| \lesssim \frac{3}{2} \times \Delta a_{CP}^{\text{dir}} = 0.4\%. \quad (49)$$

This estimate assumes that two matrix elements corresponding to different $SU(3)_F$ representations are similar in magnitude. We remark that there is no strict correlation between $a_{CP}^{\text{dir}}(D^0 \rightarrow K_S K_S)$ and $\Delta a_{CP}^{\text{dir}}$, because the two quantities involve different topological amplitudes.

VI. CONCLUSIONS

We have studied the direct and mixing-induced CP asymmetries in $D^0 \rightarrow K_S K_S$ in the Standard Model.

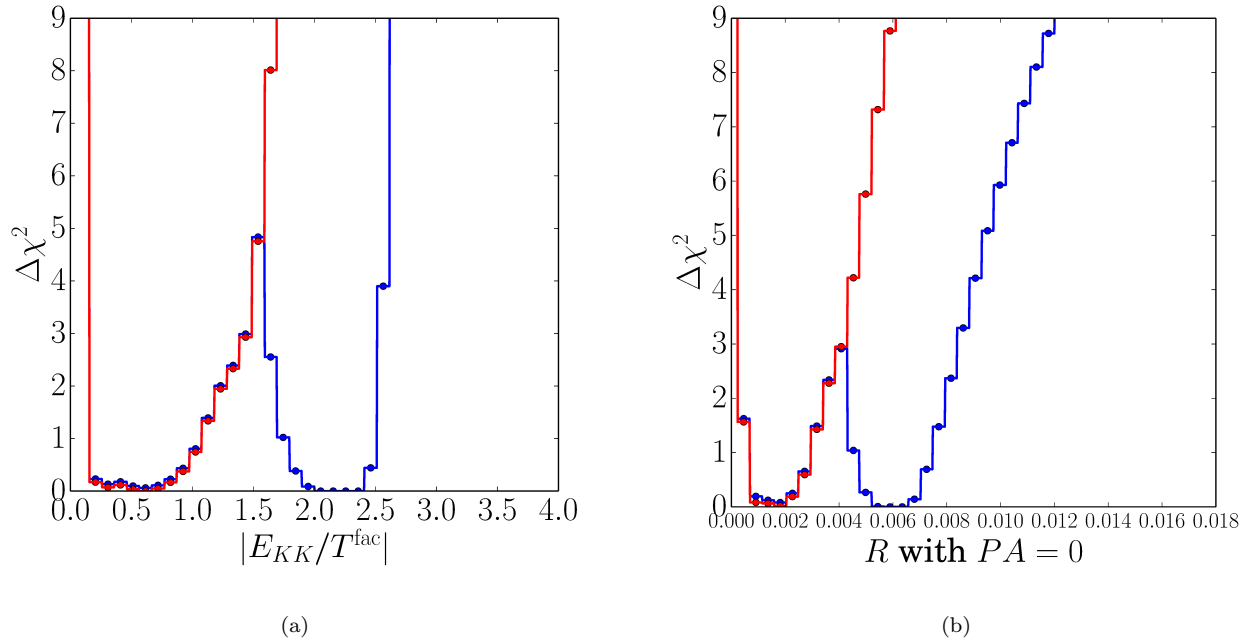


FIG. 2. (a) $\Delta\chi^2$ profile of $|E_{KK}|$. (b) $\Delta\chi^2$ profile of R (defined in Eq. (22)) for $PA = 0$. The blue and red curves correspond to the scenarios without and with $1/N_c$ counting applied to C and E . Note that the red line lies partially on top of the blue line.

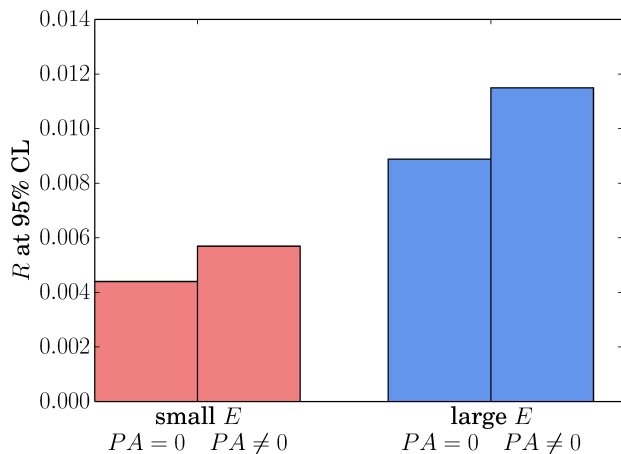


FIG. 3. Theoretical upper bounds on R . Predictions with (without) $1/N_c$ counting are labeled “small E ” (“large E ”). To visualize the contribution from exchange diagrams, we also show the result for $PA = 0$. The case $PA \neq 0$ is based on the estimate in Eq. (40).

The allowed region for the corresponding two quantities a_{CP}^{dir} and $\phi - \phi^{\text{mix}}$ is a disc whose radius can be calculated in terms of the exchange amplitude E_{KK} and the penguin annihilation amplitude PA . We estimate PA/E_{KK} with

a perturbative calculation and obtain E_{KK} from a global fit to D branching fractions as described in Ref. [16]. We find

$$|a_{CP}^{\text{dir}}| \leq 1.1\% \quad (95\% \text{ C.L.}), \quad (50)$$

$$|\phi - \phi_{\text{mix}} + \text{Im} \frac{\lambda_b}{\lambda_{sd}}| \leq 1.1\% \quad (95\% \text{ C.L.}). \quad (51)$$

A simultaneous measurement of a_{CP}^{dir} and $\phi - \phi_{\text{mix}}$ will determine $|2E_{KK} + PA|$. A violation of the bound

$$\sqrt{a_{CP}^{\text{dir}2} + \left(\phi - \phi_{\text{mix}} + \text{Im} \frac{\lambda_b}{\lambda_{sd}}\right)^2} \leq 1.1\%$$

will point to an anomalously enhanced PA . In this case other CP asymmetries will also be enhanced.

Note added in Proof: The authors of Ref. [14] have informed us that they agree with our expression Eq. (41). The apparent difference is due to a typo in Eq. (13) of Ref. [14]. By comparing our numerical codes we could trace our numerical differences back to the “ $i\epsilon$ problem” mentioned at the end of Sec. IV.

ACKNOWLEDGMENTS

We thank Philipp Frings and Tim Gershon for useful discussions and the authors of Ref. [14] for a thorough comparison of the penguin loop function. UN and StS

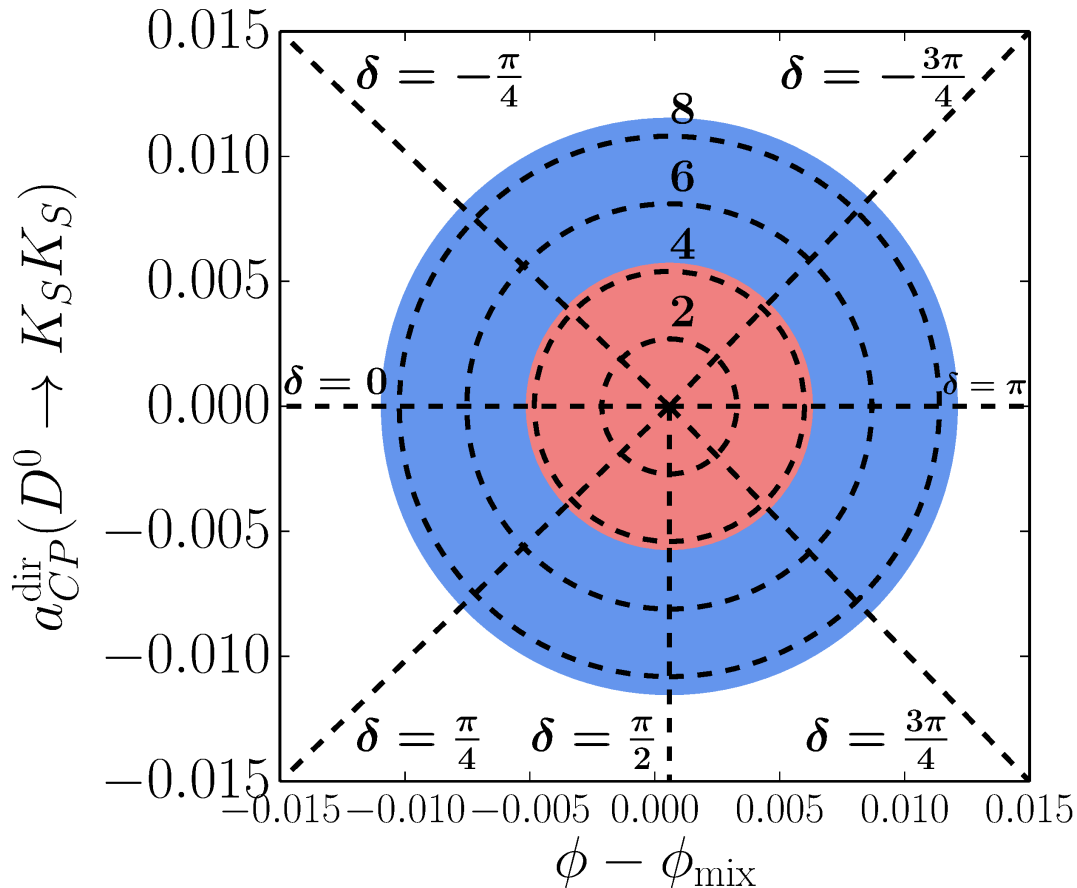


FIG. 4. Correlation of direct and mixing-induced CPV for $D^0 \rightarrow K_S K_S$ from Eqs. (23) to (25). The one-dimensional 95% C.L. ($\Delta\chi^2 = 3.84$) upper limits on $a_{CP}^{\text{dir}}(D^0 \rightarrow K_S K_S)$ and $\phi - \phi_{\text{mix}}$ are shown in blue. If in addition $1/N_c$ counting is applied to the topological amplitudes C and E , the allowed region shrinks to the red area. The black dashed lines show the radii which are obtained when setting $|2E_{KK} + PA|/2.52 \cdot 10^{-6}$ GeV to the annotated values. The chosen reference value is the typical size of a factorized tree amplitude in D decays, $T^{\text{fac}} = 2.52 \cdot 10^{-6}$ GeV. Further, for the black dashed lines $\mathcal{B}(D^0 \rightarrow K_S K_S) = 0.17 \cdot 10^{-3}$ is used. The circle is centered at $(-\text{Im}(\lambda_b)/\lambda_{sd}, 0) = (6 \cdot 10^{-4}, 0)$.

acknowledge the kind hospitality of the *Munich Institute for Astro- and Particle Physics*. The fits are performed using the `python` version of the software package

`myFitter` [40]. The Feynman diagrams are drawn using `Jaxodraw` [41, 42]. The presented work is supported by BMBF under contract no. 05H15VKKB1.

[1] V. Fanti *et al.* (NA48), Phys. Lett. **B465**, 335 (1999), arXiv:hep-ex/9909022 [hep-ex].
[2] A. Lai *et al.* (NA48), Eur. Phys. J. **C22**, 231 (2001), arXiv:hep-ex/0110019 [hep-ex].
[3] J. R. Batley *et al.* (NA48), Phys. Lett. **B544**, 97 (2002), arXiv:hep-ex/0208009 [hep-ex].
[4] A. Alavi-Harati *et al.* (KTeV), Phys. Rev. Lett. **83**, 22 (1999), arXiv:hep-ex/9905060 [hep-ex].
[5] A. Alavi-Harati *et al.* (KTeV), Phys. Rev. **D67**, 012005 (2003), [Erratum: Phys. Rev.D70,079904(2004)], arXiv:hep-ex/0208007 [hep-ex].
[6] S. W. Lin *et al.* (Belle), Nature **452**, 332 (2008).
[7] Y. T. Duh *et al.* (Belle), Phys. Rev. **D87**, 031103 (2013),

arXiv:1210.1348 [hep-ex].
[8] B. Aubert *et al.* (BaBar), Phys. Rev. Lett. **99**, 021603 (2007), arXiv:hep-ex/0703016 [HEP-EX].
[9] J. P. Lees *et al.* (BaBar), Phys. Rev. **D87**, 052009 (2013), arXiv:1206.3525 [hep-ex].
[10] A. Abulencia *et al.* (CDF), Phys. Rev. Lett. **97**, 211802 (2006), arXiv:hep-ex/0607021 [hep-ex].
[11] T. Aaltonen *et al.* (CDF), Phys. Rev. Lett. **106**, 181802 (2011), arXiv:1103.5762 [hep-ex].
[12] F. Buccella, M. Lusignoli, G. Miele, A. Pugliese, and P. Santorelli, Phys.Rev. **D51**, 3478 (1995), arXiv:hep-ph/9411286 [hep-ph].
[13] B. Bhattacharya and J. L. Rosner, Phys. Rev. **D81**,

- 014026 (2010), arXiv:0911.2812 [hep-ph].
- [14] J. Brod, A. L. Kagan, and J. Zupan, Phys.Rev. **D86**, 014023 (2012), arXiv:1111.5000 [hep-ph].
- [15] G. Hiller, M. Jung, and S. Schacht, Phys.Rev. **D87**, 014024 (2013), arXiv:1211.3734 [hep-ph].
- [16] S. Müller, U. Nierste, and S. Schacht, Phys.Rev. **D92**, 014004 (2015), arXiv:1503.06759 [hep-ph].
- [17] Y. Grossman and Y. Nir, JHEP **1204**, 002 (2012), arXiv:1110.3790 [hep-ph].
- [18] M. Gersabeck, M. Alexander, S. Borghi, V. V. Glig-
orov, and C. Parkes, J. Phys. **G39**, 045005 (2012),
arXiv:1111.6515 [hep-ex].
- [19] Y. Grossman, A. L. Kagan, and Y. Nir, Phys.Rev. **D75**,
036008 (2007), arXiv:hep-ph/0609178 [hep-ph].
- [20] Y. Amhis *et al.* (Heavy Flavor Averaging Group), (2012),
arXiv:1207.1158, and online update 30 June 2014 [hep-
ex].
- [21] J. Beringer *et al.* (Particle Data Group), Phys.Rev. **D86**,
010001 (2012), and 2013 partial update for the 2014 edi-
tion.
- [22] R. Aaij *et al.* (LHCb collaboration), JHEP **1407**, 041
(2014), arXiv:1405.2797 [hep-ex].
- [23] R. Aaij *et al.* (LHCb), JHEP **1504**, 043 (2015),
arXiv:1501.06777 [hep-ex].
- [24] G. Bonvicini *et al.* (CLEO Collaboration), Phys.Rev.
D63, 071101 (2001), arXiv:hep-ex/0012054 [hep-ex].
- [25] M. Alexander for the LHCb collaboration, Talk at the
European Physical Society Conference on High Energy
Physics 2015, 22-29 July 2015, Vienna, Austria, LHCb-
PAPER-2015-030, arXiv:1508.06087.
- [26] S. Müller, U. Nierste, and S. Schacht, (2015),
arXiv:1506.04121 [hep-ph].
- [27] M. Golden and B. Grinstein, Phys.Lett. **B222**, 501
(1989).
- [28] D. Pirtskhalava and P. Uttayarat, Phys.Lett. **B712**, 81
(2012), arXiv:1112.5451 [hep-ph].
- [29] D. Atwood and A. Soni, PTEP **2013**, 0903B05 (2013),
arXiv:1211.1026 [hep-ph].
- [30] M. Bander, D. Silverman, and A. Soni, Phys. Rev. Lett.
43, 242 (1979).
- [31] M. Beneke, G. Buchalla, M. Neubert, and C. T.
Sachrajda, Phys. Rev. Lett. **83**, 1914 (1999), arXiv:hep-
ph/9905312 [hep-ph].
- [32] M. Beneke, G. Buchalla, M. Neubert, and C. T. Sachra-
jda, Nucl.Phys. **B606**, 245 (2001), arXiv:hep-ph/0104110
[hep-ph].
- [33] M. Beneke and M. Neubert, Nucl. Phys. **B675**, 333
(2003), arXiv:hep-ph/0308039 [hep-ph].
- [34] M. Beneke, T. Feldmann, and D. Seidel, Eur. Phys. J.
C41, 173 (2005), arXiv:hep-ph/0412400 [hep-ph].
- [35] P. Frings, U. Nierste, and M. Wiebusch, (2015),
arXiv:1503.00859 [hep-ph].
- [36] A. Lenz, U. Nierste, and G. Ostermaier, Phys. Rev. **D56**,
7228 (1997), arXiv:hep-ph/9706501 [hep-ph].
- [37] G. 't Hooft, Nucl.Phys. **B72**, 461 (1974).
- [38] A. Buras, J. Gerard, and R. Ruckl, Nucl.Phys. **B268**,
16 (1986).
- [39] A. J. Buras and L. Silvestrini, Nucl.Phys. **B569**, 3 (2000),
arXiv:hep-ph/9812392 [hep-ph].
- [40] M. Wiebusch, Comput.Phys.Commun. **184**, 2438 (2013),
arXiv:1207.1446 [hep-ph].
- [41] D. Binosi and L. Theussl, Comput.Phys.Commun. **161**,
76 (2004), arXiv:hep-ph/0309015 [hep-ph].
- [42] J. Vermaseren, Comput.Phys.Commun. **83**, 45 (1994).